Spatial, Temporal and Comparative Analysis of Land Surface Temperature in the Southern and Central Zones of Plateau State, Nigeria (1995–2025)

Boyi Mairiga[1], Dr. Nannim Sunday[2], Kalip Amos Dindul[3], Gyang Yusuf Davou[4], Abu Ephraim[5], Gwamzhi Ponsah Emmanuel[6]

Zonal Advanced Space Technology Application Laboratory, Langtang

DOI: https://doi.org/10.47772/IJRISS.2026.100800233

Received: 19 August 2026; Accepted: 24 August 2026; Published: 01 September 2026

ABSTRACT

Land Surface Temperature (LST) is a critical indicator for assessing environmental change, climate variability, urbanization, and ecosystem health. This study presents a comparative spatio-temporal analysis of LST dynamics between the Central and Southern zones of Plateau State, Nigeria, over a 30-year period (1995–2025). The relationships between LST and Land Use/Land Cover (LULC), the Normalized Difference Vegetation Index (NDVI), and the Normalized Difference Built-up Index (NDBI) were examined to determine the influence of land-cover change on surface-temperature variation.

Landsat 7 ETM+ imagery for 1995 and 2010 and Landsat 8 OLI/TIRS imagery for 2025, each with less than 10% scene cloud cover, were obtained from the USGS EarthExplorer archive and processed in ArcGIS 10.5. Standard remote-sensing procedures were applied to convert digital numbers to spectral radiance, at-sensor brightness temperature, and land surface temperature, while supervised classification was used to generate LULC maps and NDVI/NDBI were computed using established spectral-index equations. Comparative trend analysis was performed to evaluate temporal and spatial variation between the two zones, and a preliminary correlation analysis of zonal mean LST against NDVI and NDBI was carried out to test the expected direction of association.

The results show substantial land-use change in both zones, characterized by continuous expansion of built-up land, increasing agricultural activity, and fragmentation of forest and vegetation cover. Mean LST rose markedly between 1995 and 2010 in both zones before declining slightly by 2025. The Central zone recorded mean LST of 26.89 °C, 34.33 °C, and 33.28 °C for 1995, 2010, and 2025 respectively, while the Southern zone recorded 17.62 °C, 35.51 °C, and 31.65 °C over the same period, indicating a markedly stronger thermal increase in the Southern zone between 1995 and 2010.

Areas with high NDBI consistently coincided with elevated surface temperature, whereas areas with high NDVI recorded comparatively lower temperature, consistent with a positive LST–NDBI relationship and a negative LST–NDVI relationship. Descriptive correlation of the three-period zonal means yielded negative LST–NDVI and LST–NDBI associations in both zones (Central: $r = -0.61$ and $r = -0.38$; Southern: $r = -0.98$ and $r = -0.98$, respectively), although with only three temporal observations per zone these coefficients are indicative rather than statistically conclusive and are reported here as a preliminary check on the expected direction of the relationship, pending pixel-based correlation analysis.

The study concludes that urban expansion, agricultural intensification, and vegetation loss are the principal drivers of rising land surface temperature in both the Central and Southern zones of Plateau State. The research provides baseline information for environmental monitoring, climate-change adaptation, urban planning, ecosystem conservation, and sustainable land-use management in the state. The integration of LST, NDVI, NDBI, and LULC analysis offers a replicable geospatial framework for identifying thermal hotspots and supporting evidence-based decision-making for sustainable regional development.

Keywords: Land Use/Land Cover; Normalized Difference Built-up Index; Normalized Difference Vegetation Index; Land Surface Temperature; Plateau State

INTRODUCTION

Land Surface Temperature (LST) is one of the most important indicators of environmental and climatic conditions because it reflects the thermal state of the Earth's surface. It influences several environmental processes, including evapotranspiration, soil moisture, vegetation health, hydrological cycles, and ecosystem functioning. Variations in LST are driven primarily by changes in land use and land cover (LULC), vegetation density, urbanization, topography, and climate variability. Remote sensing, and particularly Landsat satellite imagery, has become an effective tool for monitoring LST over long periods because it provides consistent, reliable, and spatially extensive observations (Odunuga & Badru, 2015).

Globally, increasing urbanization, deforestation, agricultural expansion, and climate change have significantly altered surface temperature, giving rise to environmental challenges such as Urban Heat Islands (UHIs), biodiversity loss, declining agricultural productivity, and increased heat stress (Mohamed, Lorestani & Shebani, 2025; Zhang, Hu & Yang, 2025; Vanlalchhuanga, Lawmchullova & Biswas, 2025). These changes make continuous monitoring of LST essential for sustainable environmental management and climate adaptation.

Plateau State, located in north-central Nigeria, possesses unique environmental characteristics owing to its high elevation, relatively cool climate, and diverse vegetation. The state comprises northern, central, and southern zones with varying topography, land-use practices, population density, and climatic conditions. Over the last three decades, rapid urban expansion, agricultural intensification, mining activity, vegetation degradation, and infrastructural development have altered land cover across much of the state, with potential effects on the spatial and temporal pattern of land surface temperature (Ogunro & Owolabi, 2023).

The Southern and Central zones of Plateau State are particularly important because they contain extensive agricultural land, rapidly growing settlements, forests, wetlands, and rocky landscapes. These contrasting land-cover types produce considerable spatial variation in thermal characteristics. Understanding how LST has changed between 1995 and 2025 provides insight into the impacts of land-cover change and climate variability on the region's environment (Bharambe et al., 2024; Tamrakar & Sharma, 2024). A spatial, temporal, and comparative assessment of LST using multi-temporal Landsat imagery, together with NDVI and NDBI, reveals the magnitude, direction, and distribution of thermal change across the two zones and supports evidence-based land-use planning, climate adaptation, environmental conservation, and sustainable development policy in Plateau State.

Although Plateau State has traditionally experienced relatively cool temperatures because of its high altitude, recent environmental changes, rapid urban growth, agricultural expansion, mining, and deforestation, have altered the natural landscape and potentially increased surface temperature. Despite these changes, comprehensive research comparing long-term LST variation between the Southern and Central zones of Plateau State over a 30-year period (1995–2025) remains limited. Most previous studies have focused on selected urban areas or broader regional analyses without providing a detailed spatial comparison between these two zones, so the extent, spatial distribution, and temporal dynamics of LST change in the study area remain inadequately understood. This study addresses that gap by (i) mapping LULC, NDVI, NDBI, and LST for the Central and Southern zones in 1995, 2010, and 2025; (ii) quantifying temporal trends and comparing the two zones; and (iii) evaluating the association between LST and vegetation/built-up conditions as a basis for identifying thermal hotspots.

Study Area

The Central and Southern zones of Plateau State comprise eleven (11) Local Government Areas (LGAs), namely Bokkos, Kanam, Kanke, Langtang South, Langtang North, Mangu, Mikang, Qua'an Pan, Shendam, Pankshin, and Wase. The study area covers a total land area of approximately 20,411 km² and had a population of about 1,908,179 at the 2006 national census. The area lies approximately between latitudes 8°21'50.885″N and 9°46'24.955″N and longitudes 8°38'23.358″E and 10°38'28.662″E. The elevated Jos Plateau, in the Central zone, rises to over 1,200 m above sea level; its orographic influence sustains a near-temperate microclimate with mean annual temperature of 18–25 °C. The Southern zone, in contrast, descends into the low-lying savanna transition belt, where higher ambient temperatures prevail. The area experiences a tropical climate with distinct wet and dry seasons, an annual temperature range of about 17–38 °C, and mean annual rainfall of roughly 1,324–1,500 mm (NIMET, 2018). Mean annual relative humidity exceeds 80%, peaking above 85% in July–August and falling to about 60% in January. Two broad seasonal regimes are recognized: a warm, humid period (April–October) and a cooler harmattan period (December–February) (Adesiku et al., 2020).

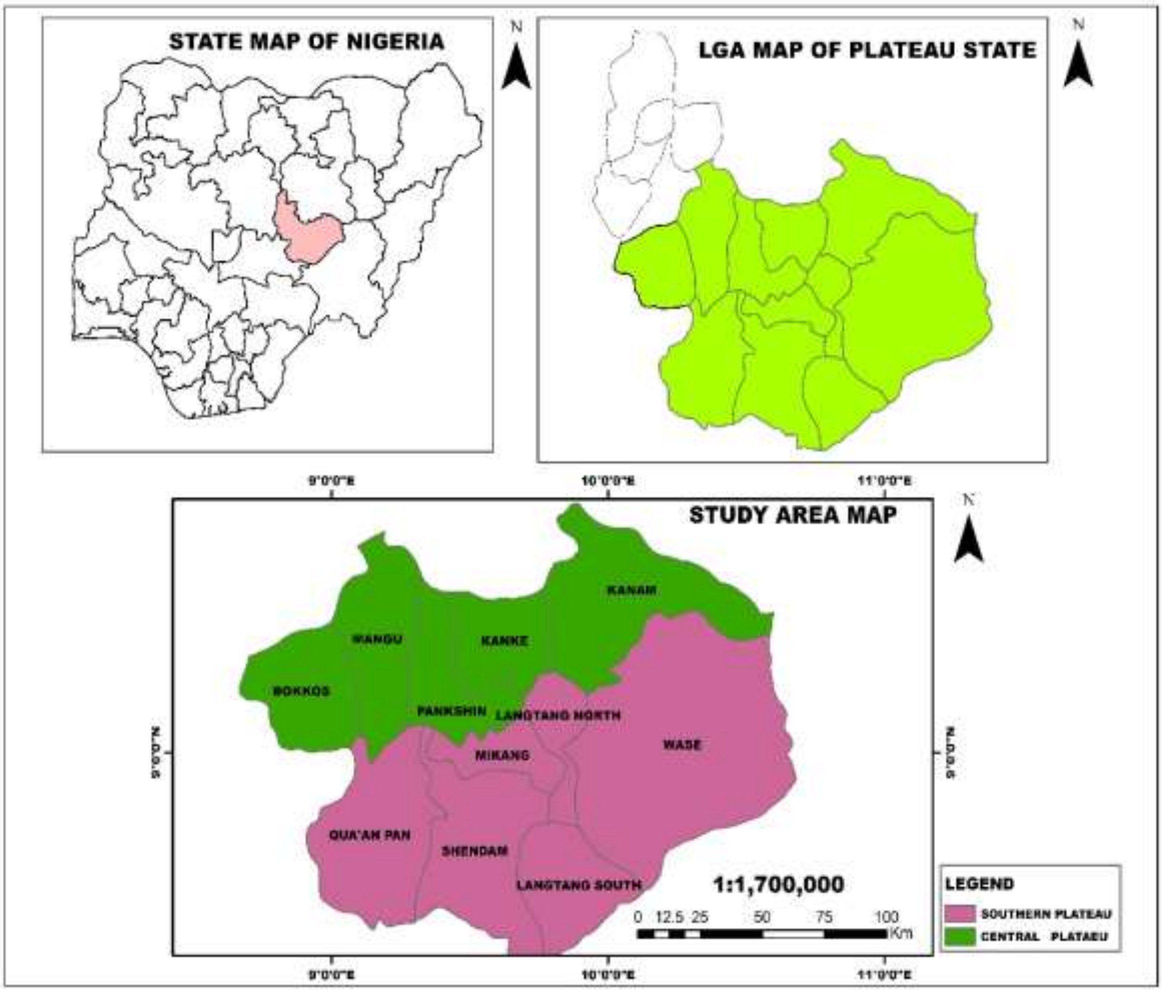

Figure 1: The Study Area

MATERIALS AND METHODS

Data Sources and Pre-Processing

Three Landsat scenes covering the Central and Southern zones of Plateau State were obtained from the United States Geological Survey (USGS) EarthExplorer archive: a Landsat 7 ETM+ scene acquired on 30 June 1995, a Landsat 7 ETM+ scene acquired on 20 June 2010, and a Landsat 8 OLI/TIRS scene acquired on 12 June 2025 (Table 1). All three scenes are historical, archived satellite observations retrieved after their respective acquisition dates; the 2025 scene reflects an actual overpass already held in the USGS archive at the time of data acquisition for this study, and not a projected or simulated future condition. Dry-season, near-anniversary dates (June, at the onset of the rains) were selected for all three periods to minimize the confounding influence of seasonal phenology and cloud cover on the comparison. Scenes with less than 10% total cloud cover, as reported in the associated metadata, were prioritized during selection, and residual cloud and cloud-shadow pixels were screened out prior to LST retrieval using the quality-assessment procedure described in Section 2.8. All processing was carried out in ArcGIS 10.5 using the standard Landsat Level-1 processing chain (digital number → spectral radiance → brightness temperature → land surface temperature).

Table 1: Landsat data used

Sensor	Acquisition Date	Path/Source
Landsat 7 ETM+	30 June 1995	USGS EarthExplorer
Landsat 7 ETM+	20 June 2010	USGS EarthExplorer
Landsat 8 OLI/TIRS	12 June 2025	USGS EarthExplorer

Conversion to Spectral Radiance

Digital numbers (DN) were converted to at-sensor spectral radiance separately for the Landsat 7 ETM+ and Landsat 8 OLI thermal bands.

For Landsat 7:

$$L\lambda = ((LMAX\lambda - LMIN\lambda) / (QCALMAX - QCALMIN)) \times (QCAL - QCALMIN) + LMIN\lambda$$

where Lλ is spectral radiance at the sensor aperture (W m^{-2} sr^{-1} μm^{-1}); QCAL is the quantized calibrated pixel value (DN); LMINλ and LMAXλ are the spectral radiance scaled to QCALMIN and QCALMAX respectively; QCALMIN is the minimum quantized pixel value and QCALMAX the maximum quantized pixel value (255 for 8-bit ETM+ data).

For Landsat 8:

$$L\lambda = ML \times Qcal + AL$$

where Lλ is spectral radiance (W m^{-2} sr^{-1} μm^{-1}); ML is the band-specific radiance multiplicative scaling factor (RADIANCE_MULT_BAND_n); AL is the band-specific radiance additive scaling factor (RADIANCE_ADD_BAND_n); and Qcal is the Level-1 pixel value (DN). Both ML and AL were obtained from each scene's metadata (MTL) file.

Conversion to At-Sensor Brightness Temperature

Spectral radiance was converted to at-sensor (top-of-atmosphere) brightness temperature, the effective temperature that would be observed by the satellite under an assumption of unit surface emissivity, using:

$$T = \frac{K2}{\ln\left(\frac{K1}{L_\lambda} + 1\right)}$$

where T is the top-of-atmosphere brightness temperature (K); Lλ is spectral radiance (W m^{-2} sr^{-1} μm^{-1}); and K1 and K2 are the thermal-band conversion constants (K1_CONSTANT_BAND_n and K2_CONSTANT_BAND_n) obtained from each scene's metadata file.

Land Surface Temperature Retrieval

For Landsat 7, brightness temperature was converted from Kelvin to degrees Celsius:

$$LST = T(K) - 273.15$$

ISSN No. 2454-6186 | DOI: 10.47772/IJRISS | Volume X Issue VIII August 2026

For Landsat 8, LST was additionally corrected for surface emissivity (Section 2.5) using:

$$LST = (BT / 1) + W \times (BT / 14380) \times \ln(\varepsilon)$$

where BT is the top-of-atmosphere brightness temperature (°C); W is the wavelength of emitted radiance (11.5 µm for Landsat 8 Band 10); and ε is land surface emissivity.

Land Surface Emissivity and Vegetation Proportion

Land surface emissivity (LSE), the average emissivity of a surface element, was derived from the Normalized Difference Vegetation Index (NDVI) using the vegetation-proportion (Pv) method:

$$Pv = [(NDVI - NDVImin) / (NDVImax - NDVImin)]^2$$

where Pv is the proportion of vegetation, and NDVImin and NDVImax are the minimum and maximum NDVI values in the image. Emissivity was then estimated as:

$$\varepsilon = 1.0094 + 0.0047 \ln(Pv)$$

Normalized Difference Vegetation Index (NDVI)

NDVI is a widely used index of vegetation condition, ranging from −1 to +1, that indicates vegetation health, phenology, and extent. It was computed as:

$$NDVI = (NIR - RED) / (NIR + RED)$$

where NIR corresponds to Band 4 in Landsat TM/ETM+ (0.76–0.90 µm) and Band 5 in Landsat OLI (0.85–0.88 µm), and RED corresponds to Band 3 in Landsat TM/ETM+ (0.63–0.69 µm) and Band 4 in Landsat OLI (0.64–0.67 µm).

Normalized Difference Built-up Index (NDBI)

NDBI, derived from reflectance in the red and mid-infrared (MIR) portions of the spectrum, was computed as:

$$NDBI = (MIR - RED) / (MIR + RED)$$

Positive NDBI values indicate built-up and other impervious surfaces, while negative values are typically associated with vegetation, water, and other natural land covers.

Atmospheric Correction and Cloud Screening

Prior to spectral-index and LST computation, each scene was screened for cloud, cloud-shadow, and sensor-error pixels using the quality-assessment (QA) band distributed with the Landsat Level-1 product; flagged pixels were excluded from subsequent zonal statistics. Scene selection itself (Section 2.1) already limited analysis to imagery with less than 10% total cloud cover, so the additional QA-based mask affected only a small fraction of pixels concentrated at scene margins. Atmospheric scattering and absorption in the visible and near-infrared bands, which can bias NDVI and NDBI if uncorrected, were minimized by using top-of-atmosphere reflectance products together with consistent, near-anniversary-date, dry-season image selection across all three epochs, which reduces the influence of seasonal atmospheric variability on the cross-date comparison. We note this as a methodological simplification relative to a full radiative-transfer (e.g., 6S) atmospheric correction: because such a correction was not applied pixel-by-pixel in the present analysis, absolute NDVI/NDBI/LST values for a single date should be interpreted with some caution, even though the relative, cross-zone and cross-date comparisons that this study relies on are considerably more robust to this simplification than absolute values would be.

ISSN No. 2454-6186 | DOI: 10.47772/IJRISS | Volume X Issue VIII August 2026

Land Use/Land Cover Classification

LULC maps for 1995, 2010, and 2025 were produced by supervised classification of each Landsat scene into six classes: water body, forest, vegetation, built-up land, bare land, and agricultural land. Training samples for each class were digitized on-screen with reference to spectral response, texture, tone, and contextual knowledge of the study area, drawing on field familiarity with the distribution of settlements, farmland, forest reserves, and rock outcrops across the eleven LGAs. The resulting class boundaries were visually cross-checked against the corresponding NDVI and NDBI surfaces for internal consistency before the areal statistics in Tables 2 and 3 were computed.

Statistical and Comparative Analysis

Zonal minimum, maximum, and mean values of NDVI, NDBI, and LST were extracted for the Central and Southern zones in each of the three years. Temporal trends within each zone and differences between zones were evaluated descriptively (Sections 3.1–3.3), and Pearson correlation was computed between the zonal-mean LST series and the corresponding zonal-mean NDVI and NDBI series for each zone, to test whether the sign of the association is consistent with the expected negative LST–NDVI and positive LST–NDBI relationships reported in the literature (Section 3.3.5, Table 14).

Limitations

As with any single-date thermal retrieval, LST derived from Landsat imagery reflects surface conditions at the specific moment of satellite overpass and can be influenced by short-term weather, antecedent rainfall, and time-of-day effects.

The emissivity correction applied here (Section 2.5) follows the widely used NDVI-threshold approach, and atmospheric effects were controlled through careful scene selection and QA-based cloud masking (Section 2.8) rather than a full pixel-level radiative-transfer correction; this is a common and accepted simplification in comparative LULC/LST studies of this kind, and its effect on the relative, cross-zone and cross-period comparisons that are the focus of this study is expected to be modest even where it introduces some uncertainty into absolute LST values.

RESULTS AND DISCUSSION

The spatial distribution of LULC, NDBI, NDVI, and LST within the Central and Southern zones is presented in the figures and tables below, followed by a comparative analysis between the two zones and a discussion of the findings in relation to previous studies.

Central Zone

Land Use/Land Cover Trends

Figure 2 shows the LULC maps for the Central zone in 1995, 2010, and 2025 and the associated changes in water bodies, forest, vegetation, built-up land, bare land, and agricultural land over the 30-year period. Agricultural land remained the predominant land cover throughout the study period. Built-up land increased steadily from 1995 to 2025, indicating rapid urban growth and increasing human activity. Forest cover showed a gradual decline and became more fragmented owing to agricultural expansion and settlement development. Vegetation exhibited localized fluctuation, with gains in some areas and losses in others, while water bodies and bare land remained relatively stable, with only minor spatial change.

ISSN No. 2454-6186 | DOI: 10.47772/IJRISS | Volume X Issue VIII August 2026

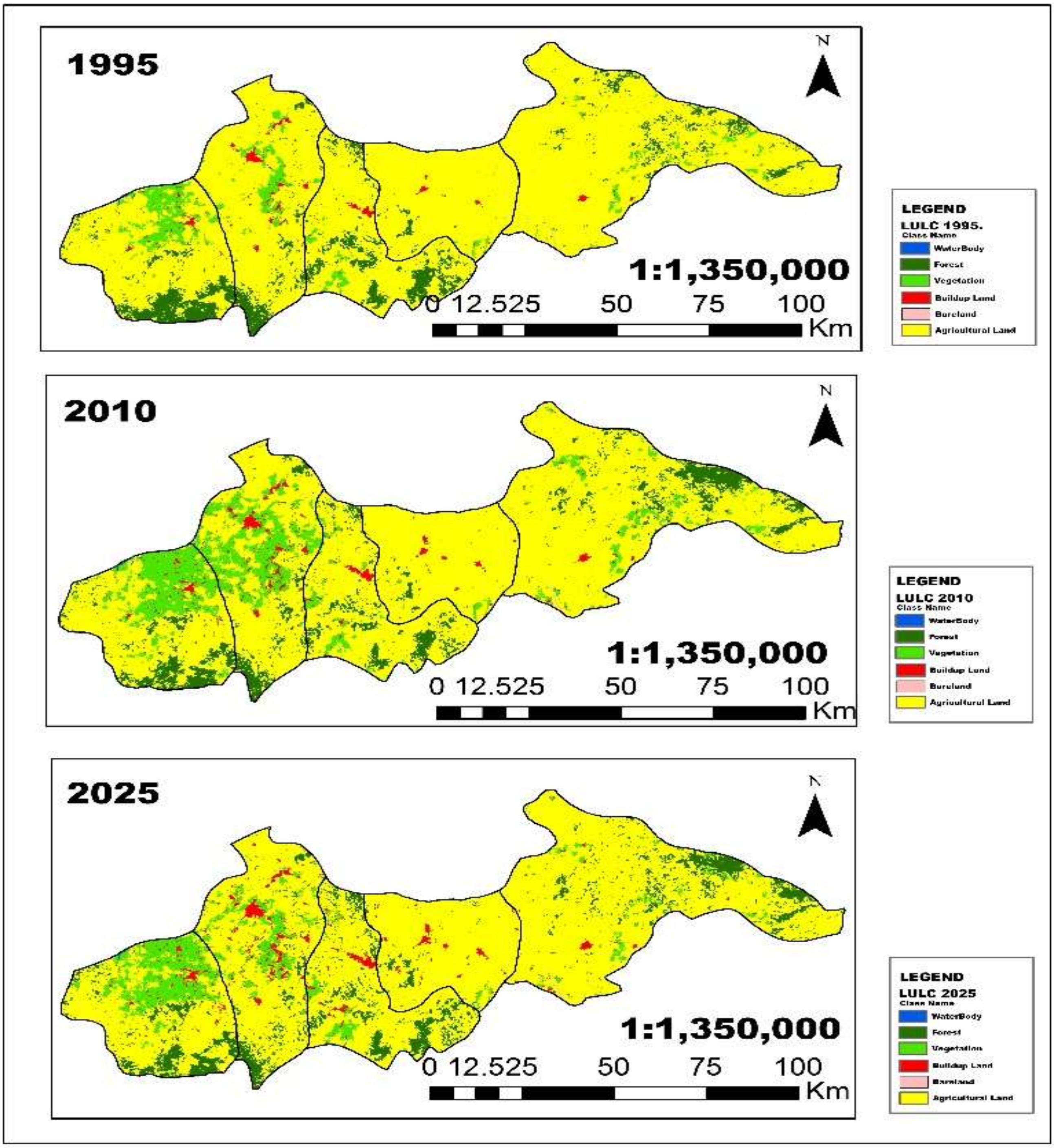

Figure 2: Land Use/Land Cover, Central Zone (1995, 2010, 2025)

NDBI Trends

The NDBI maps for the Central zone (Figure 3) show the spatial distribution and temporal change in built-up area. Positive NDBI values indicate built-up and impervious surfaces, while negative values represent vegetation, water bodies, and other natural land cover; an increase in NDBI over time generally reflects urban expansion and infrastructure development. The analysis indicates a steady increase in built-up land across the Central zone over the 30-year period, from a few isolated settlements in 1995 to more extensive and interconnected built-up areas by 2025, reflecting increasing population, economic activity, and infrastructure development. The Central zone nonetheless remains predominantly agricultural and vegetated, as indicated by the widespread low NDBI values, though the observed increase in built-up surfaces suggests growing pressure on agricultural land and natural ecosystems and underscores the need for sustainable urban planning and effective land-use management.

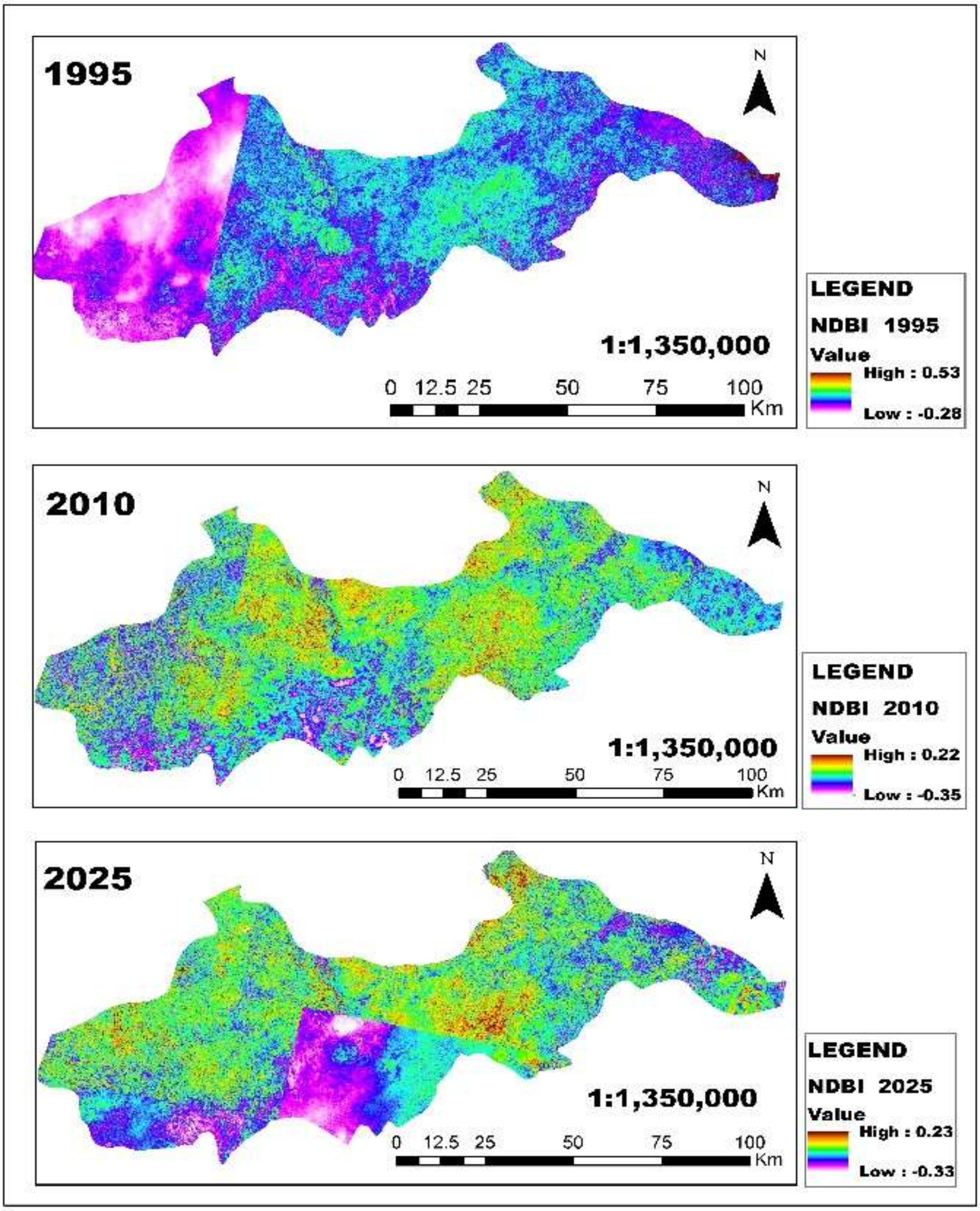

Figure 3: Normalized Difference Built-up Index, Central Zone (1995, 2010, 2025)

NDVI Trends

The NDVI maps for the Central zone (Bokkos, Mangu, Pankshin, Kanke, and Kanam LGAs; Figure 4) illustrate the spatial distribution and temporal change in vegetation health and density. Higher NDVI values (green) represent dense, healthy vegetation, while lower values (orange to red) indicate sparse vegetation, bare surfaces, or built-up areas. The Central zone maintained generally moderate vegetation cover between 1995 and 2025, with the highest vegetation density consistently occurring in Bokkos and Pankshin LGAs. While maximum NDVI increased from 0.69 in 1995 to 0.76 in 2025, the spatial distribution of vegetation became more fragmented owing to agricultural expansion, urban growth, and other land-use change; the persistence of low NDVI values in parts of Mangu, Kanke, and Kanam reflects increasing human pressure on vegetation resources.

ISSN No. 2454-6186 | DOI: 10.47772/IJRISS | Volume X Issue VIII August 2026

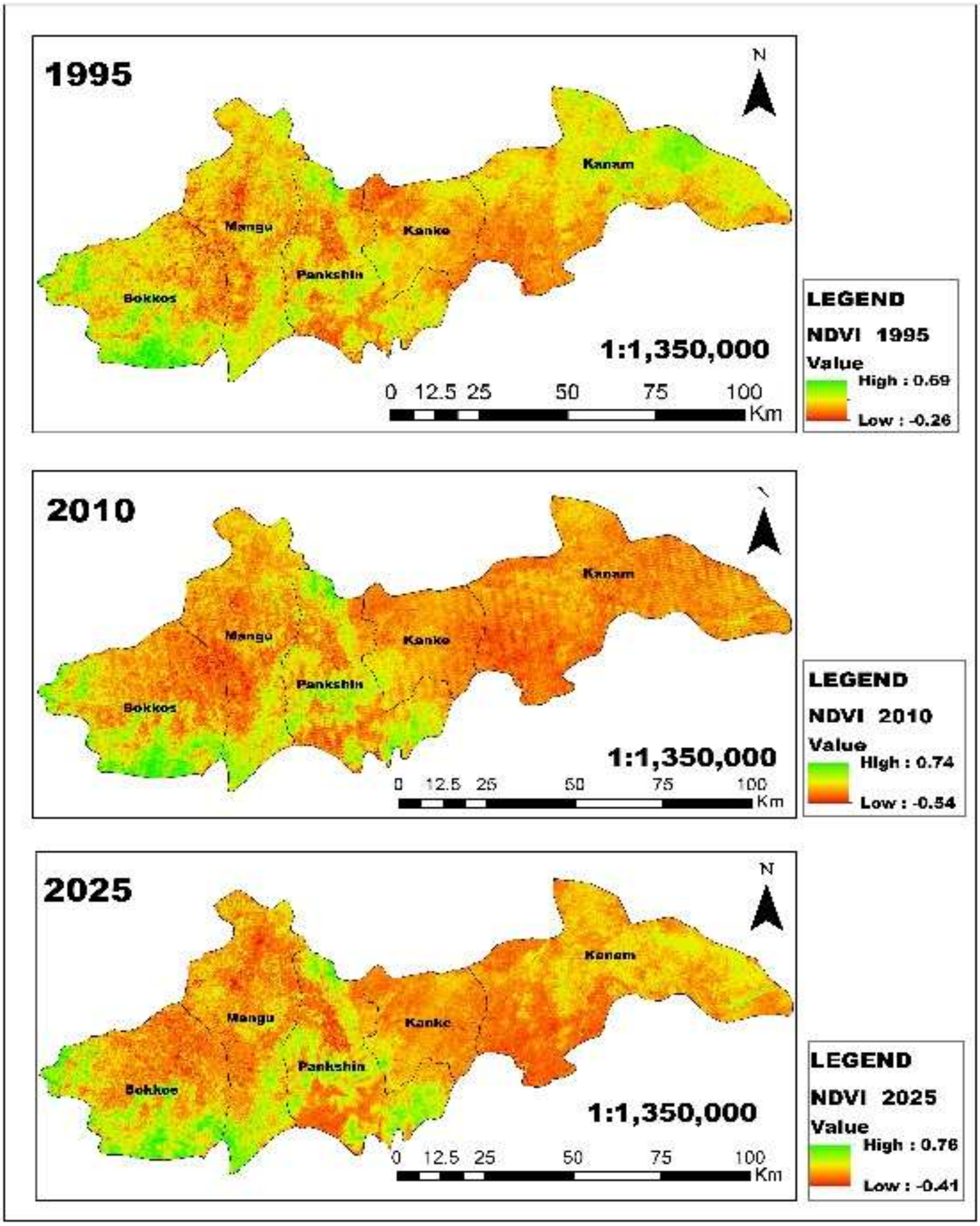

Figure 4: Normalized Difference Vegetation Index, Central Zone (1995, 2010, 2025)

LST Trends

The LST maps for the Central zone (Figure 5) illustrate spatial and temporal variation in surface temperature between 1995, 2010, and 2025. Temperature distribution is closely related to LULC characteristics, vegetation density, and built-up development: densely vegetated areas generally exhibit lower temperature, whereas agricultural land, bare surfaces, and built-up areas experience relatively higher temperature. Surface temperature increased substantially from 1995 to 2010, largely owing to agricultural expansion, urban development, vegetation loss, and increasing exposure of bare surfaces. Although maximum LST declined slightly by 2025 (43.54 °C) compared with 2010 (48.57 °C), several areas, particularly Pankshin, southern Mangu, and parts of Bokkos, continued to experience relatively high temperature, while Kanke and Kanam consistently exhibited lower temperature owing to relatively greater vegetation cover and less intensive land-use transformation.

ISSN No. 2454-6186 | DOI: 10.47772/IJRISS | Volume X Issue VIII August 2026

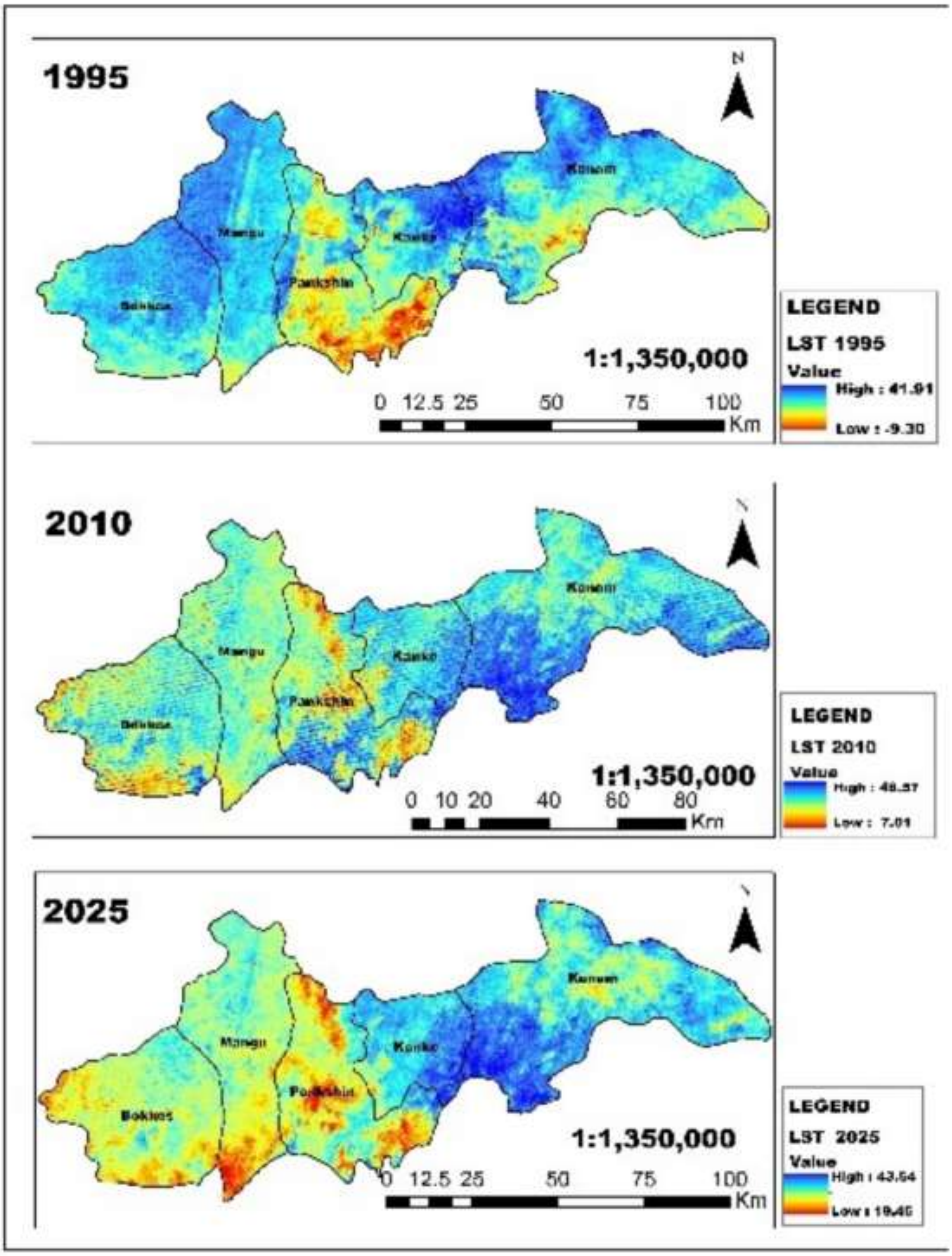

Figure 5: Land Surface Temperature, Central Zone (1995, 2010, 2025)

Southern Zone

Land Use/Land Cover Trends

The Southern zone LULC maps (Figure 6) illustrate the spatial distribution and temporal change in water bodies, forest, vegetation, built-up land, bare land, and agricultural land across Qua'an Pan, Shendam, Mikang, Langtang North, Langtang South, and Wase LGAs. The maps reveal a clear trend of increasing human influence on the landscape over the 30-year period. Agricultural land remained the dominant land-use class, supporting the predominantly agrarian economy of the Southern zone. Built-up land increased steadily, reflecting population growth, urban expansion, and infrastructure development. Forest cover gradually declined and became

ISSN No. 2454-6186 | DOI: 10.47772/IJRISS | Volume X Issue VIII August 2026

fragmented, while vegetation showed localized gains and losses depending on land-management practice and agricultural activity. Water bodies and bare land experienced minimal change over the study period.

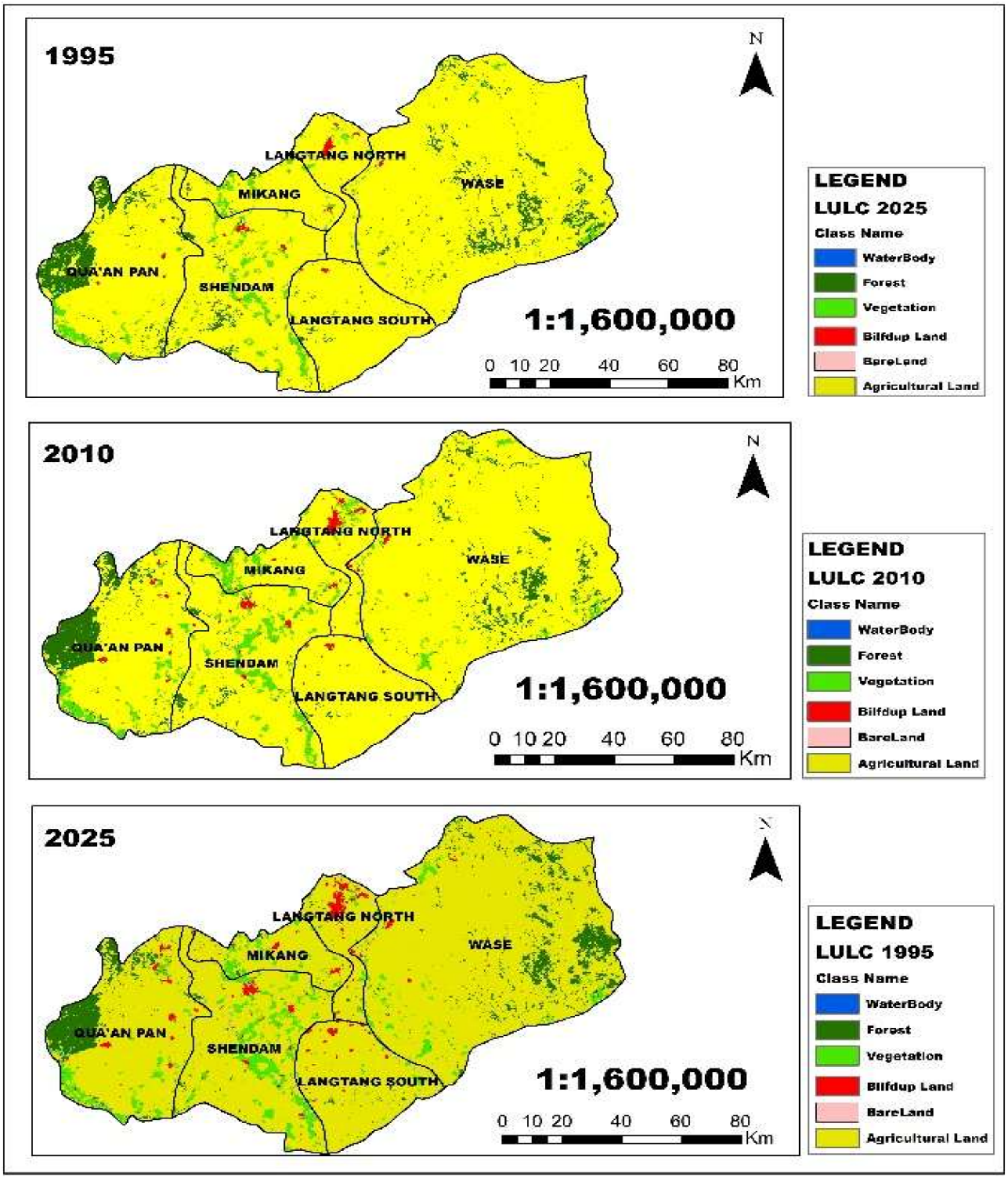

Figure 6: Land Use/Land Cover, Southern Zone (1995, 2010, 2025)

NDBI Trends

The NDBI maps for the Southern zone (Figure 7) show the spatial distribution and temporal change in built-up area across Qua'an Pan, Shendam, Mikang, Langtang North, Langtang South, and Wase LGAs. The maps indicate a progressive increase in built-up land across the Southern zone over the three decades: urban expansion was initially concentrated around established settlements and gradually spread into surrounding areas by 2025, reflecting increasing population, economic development, and infrastructure expansion. The Southern zone nonetheless remains largely characterized by agricultural land and natural vegetation, as shown by the widespread low NDBI values.

INTERNATIONAL JOURNAL OF RESEARCH AND INNOVATION IN SOCIAL SCIENCE (IJRISS)
ISSN No. 2454-6186 | DOI: 10.47772/IJRISS | Volume X Issue VIII August 2026

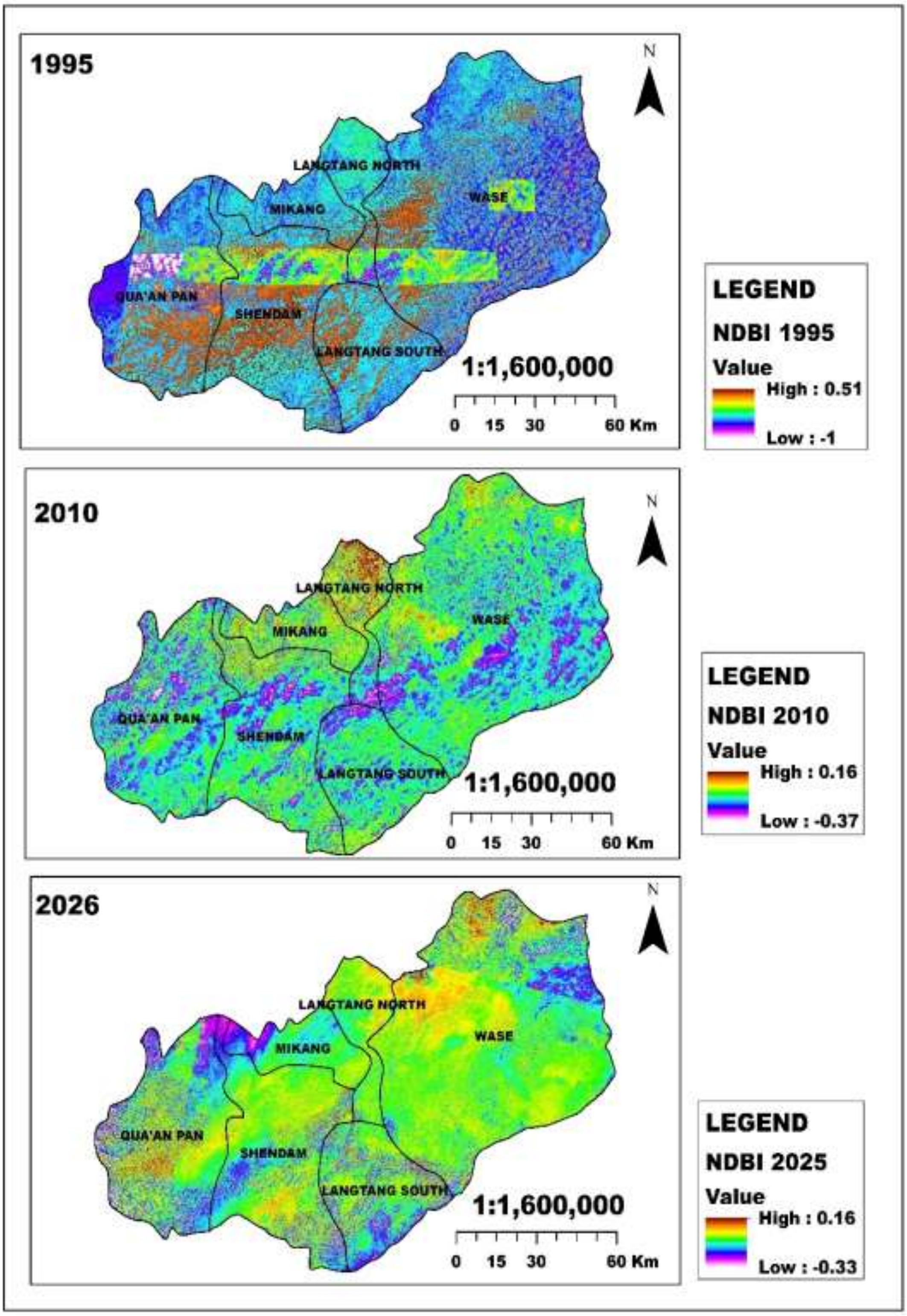

Figure 7: Normalized Difference Built-up Index, Southern Zone (1995, 2010, 2025)

NDVI Trends

The NDVI maps for the Southern zone (Qua'an Pan, Shendam, Mikang, Langtang North, Langtang South, and Wase LGAs; Figure 8) show the spatial distribution and temporal change in vegetation cover and health. The Southern zone maintained generally moderate vegetation cover between 1995 and 2025. Vegetation declined slightly between 1995 and 2010, mainly owing to agricultural expansion and increasing human activity, but the 2025 data show signs of vegetation recovery, particularly in Wase, Mikang, and Langtang North. Shendam and Langtang South, by contrast, continued to exhibit relatively lower vegetation density throughout the study period because of intensive farming and settlement development.

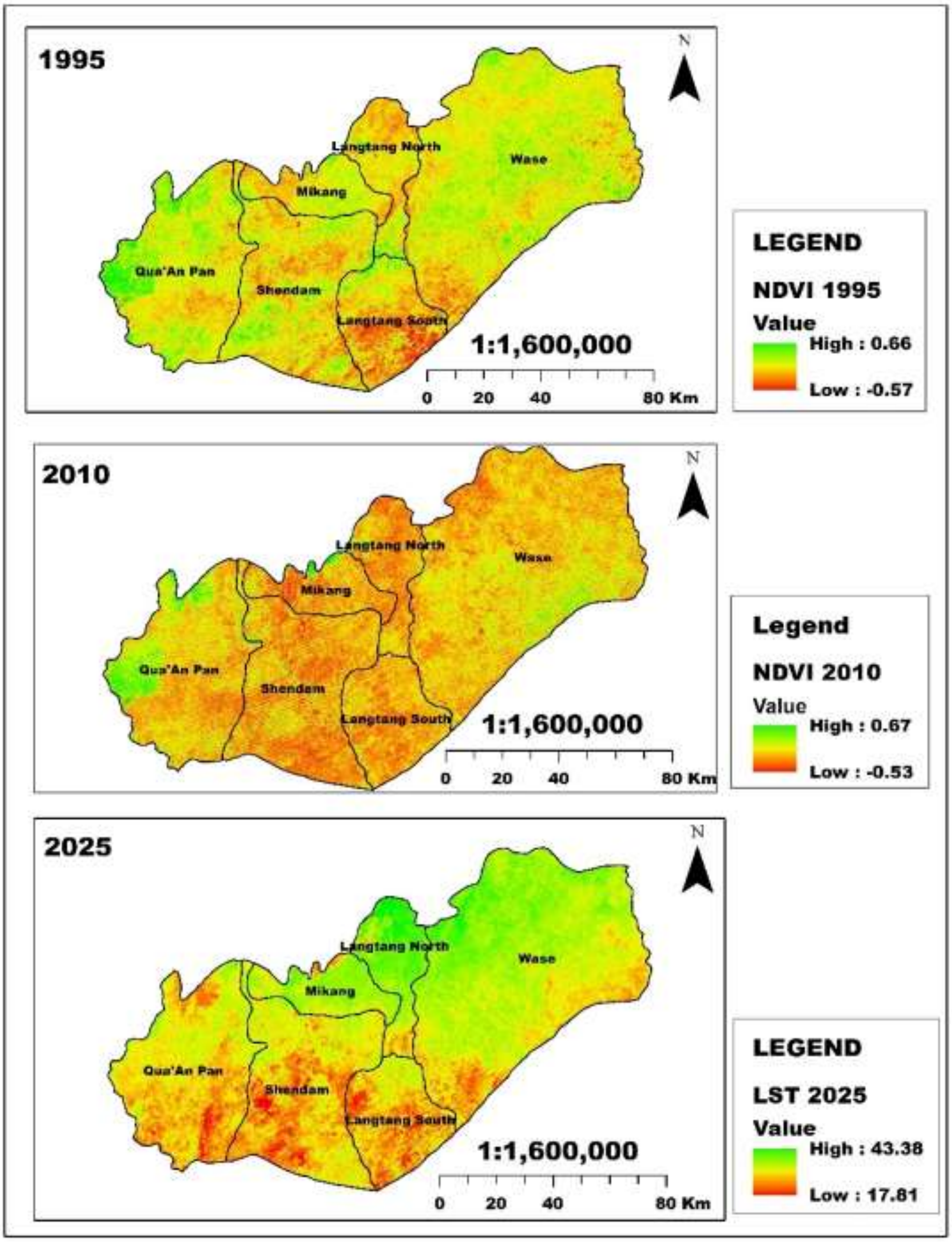

Figure 8: Normalized Difference Vegetation Index, Southern Zone (1995, 2010, 2025)

LST Trends

The LST maps for the Southern zone (Figure 9) show the spatial and temporal distribution of surface temperature over the 1995–2025 period. The observed temperature pattern is closely linked to variation in vegetation cover, LULC, agricultural activity, and settlement expansion: densely vegetated areas generally exhibit lower surface temperature, while agricultural land, bare surfaces, and built-up areas record relatively higher temperature. LST rose overall between 1995 and 2025, although the pattern varied spatially. The highest maximum temperature occurred in 2010 (48.73 °C), followed by a decline in 2025 (43.38 °C). Shendam and Langtang South consistently recorded the highest temperature throughout the study period because of intensive agricultural activity, expanding settlements, and reduced vegetation cover, whereas Wase, Langtang North, and Mikang generally maintained lower surface temperature owing to relatively dense vegetation and forest cover.

ISSN No. 2454-6186 | DOI: 10.47772/IJRISS | Volume X Issue VIII August 2026

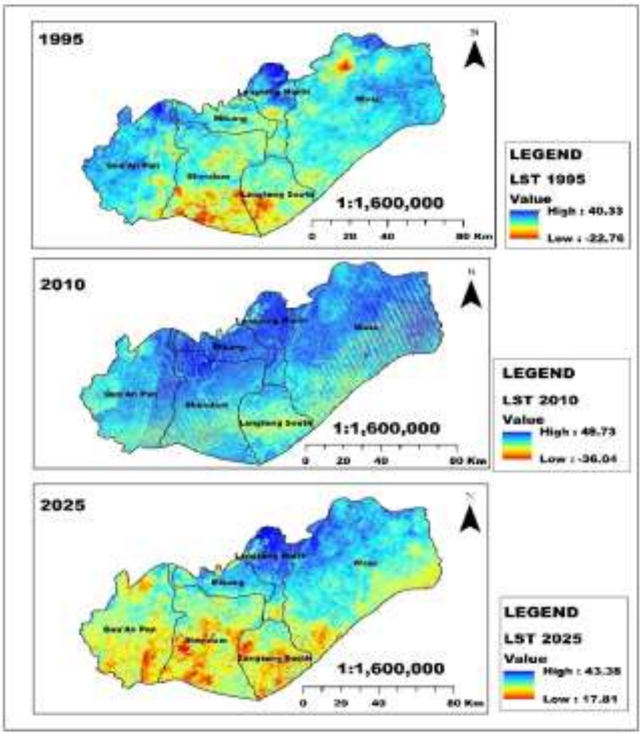

Figure 9: Land Surface Temperature, Southern Zone (1995, 2010, 2025)

Comparative Analysis Between the Central and Southern Zones

Land Use/Land Cover Comparison

Tables 2 and 3 show clear urban expansion in both zones, seen in the steady rise of built-up land from 1995 to 2025. In the Central zone, built-up land increased from 84.16 km² in 1995 to 207.34 km² in 2025, while in the Southern zone it rose from 57.92 km² to 216.83 km². Settlement growth and infrastructure development therefore intensified in both zones, with the Southern zone marginally surpassing the Central zone by 2025.

Table 2: Land Use/Land Cover area, Central Zone (km²), 1995–2025

LULC Class	1995	2010	2025
Water body	5.89	4.95	6.40
Forest	748.64	775.73	840.01
Vegetation	434.16	1073.50	766.50
Built-up land	84.16	145.04	207.34
Bare land	8.82	9.36	6.81
Agricultural land	7511.36	6897.33	7078.84

Table 3: Land Use/Land Cover area, Southern Zone (km²), 1995–2025

LULC Class	1995	2010	2025
Water body	17.00	17.94	20.59
Forest	852.17	757.85	908.22
Vegetation	470.58	772.12	869.92

Built-up land	57.92	141.04	216.83
Bare land	30.93	39.54	35.15
Agricultural land	12566.70	12461.30	12139.10

Table 4: Comparative LULC trend, Central vs. Southern Zone

LULC Class	Central Zone Trend	Southern Zone Trend
Water body	Fluctuated, slight overall increase	Steady increase
Forest	Steady increase	Declined then increased strongly
Vegetation	Sharp rise then decline	Continuous increase
Built-up land	Strong, continuous increase	Strong, continuous increase
Bare land	Slight fluctuation, overall decline	Slight fluctuation, overall increase
Agricultural land	Declined then partially recovered	Gradual, continuous decline

NDBI Comparison

Table 5: NDBI summary statistics, Central Zone

Year	Minimum NDBI	Maximum NDBI	Mean NDBI
1995	−0.285	0.531	−0.05
2010	−0.353	0.229	−0.05
2025	−0.335	0.239	−0.06

Table 6: NDBI summary statistics, Southern Zone

Year	Minimum NDBI	Maximum NDBI	Mean NDBI
1995	−1.00	0.51	−0.04
2010	−0.37	0.16	−0.09
2025	−0.33	0.16	−0.09

Tables 5 and 6 show that both zones changed between 1995, 2010, and 2025, but the Southern zone recorded a stronger decline in mean NDBI over time. In the Central zone, mean NDBI remained at −0.05 in 1995 and 2010, declining slightly to −0.06 by 2025, relatively stable conditions over the first two periods followed by a small reduction. In the Southern zone, mean NDBI fell from −0.04 in 1995 to −0.09 in 2010 and remained at −0.09 in 2025, indicating a clearer downward shift than in the Central zone, with the major change occurring between 1995 and 2010 (Table 7).

Table 7: Comparative mean NDBI, Central vs. Southern Zone

Year	Central Mean NDBI	Southern Mean NDBI	Comparison
1995	−0.05	−0.04	Southern slightly higher

2010	−0.05	−0.09	Southern declined more
2025	−0.06	−0.09	Southern remained lower

NDVI Comparison

Table 8: NDVI summary statistics, Central Zone

Year	Minimum NDVI	Maximum NDVI	Mean NDVI
1995	−0.25	0.69	0.32
2010	−0.54	0.74	0.29
2025	−0.41	0.76	0.32

Table 9: NDVI summary statistics, Southern Zone

Year	Minimum NDVI	Maximum NDVI	Mean NDVI
1995	−0.57	0.66	0.29
2010	−0.53	0.67	0.28
2025	−0.24	0.74	0.28

Tables 8 and 9 show that both zones had generally stable NDVI between 1995 and 2025, but the Central zone maintained slightly higher mean vegetation condition overall. In the Central zone, mean NDVI declined from 0.32 in 1995 to 0.29 in 2010, then recovered to 0.32 in 2025, indicating a temporary reduction in vegetation vigor around 2010 followed by recovery. In the Southern zone, mean NDVI changed only slightly, from 0.29 in 1995 to 0.28 in 2010 and 0.28 in 2025, suggesting more stable but slightly lower vegetation condition than in the Central zone throughout the study period (Table 10).

Table 10: Comparative mean NDVI, Central vs. Southern Zone

Year	Central Mean NDVI	Southern Mean NDVI	Interpretation
1995	0.32	0.29	Central slightly higher
2010	0.29	0.28	Both declined slightly
2025	0.32	0.28	Central recovered; Southern stable

LST Comparison

Table 11: LST summary statistics, Central Zone (°C)

Year	Minimum LST	Maximum LST	Mean LST
1995	−9.30	41.91	26.89
2010	7.02	48.57	34.33
2025	19.45	43.54	33.28

Table 12: LST summary statistics, Southern Zone (°C)

Year	Minimum LST	Maximum LST	Mean LST
1995	−22.76	40.34	17.62
2010	−36.04	48.73	35.51
2025	17.81	43.38	31.65

Tables 11 and 12 show LST rising sharply from 1995 to 2010 and then falling modestly by 2025 in both zones, a pattern consistent with the broader evidence that land-cover change, urbanization, vegetation loss, and built-up expansion tend to raise LST while vegetated surfaces remain comparatively cool. In the Central zone, mean LST rose from 26.89 °C in 1995 to 34.33 °C in 2010, an increase of 7.44 °C, whereas in the Southern zone mean LST rose more sharply, from 17.62 °C to 35.51 °C, an increase of 17.89 °C. This stronger Southern increase suggests more rapid thermal intensification between 1995 and 2010, although the very low minimum LST values recorded in 1995 and 2010, particularly the −22.76 °C and −36.04 °C minima in the Southern zone, should be interpreted cautiously, since remote-sensing LST retrieval can be affected by cloud contamination, data gaps, sensor/atmospheric artefacts, and processing choices at the pixel level.

From 2010 to 2025, mean LST declined slightly in both zones, from 34.33 °C to 33.28 °C in the Central zone and from 35.51 °C to 31.65 °C in the Southern zone. Maximum LST also fell in both zones, from 48.57 °C to 43.54 °C in the Central zone and from 48.73 °C to 43.38 °C in the Southern zone. This pattern suggests partial thermal moderation rather than a full return to 1995 conditions, plausibly reflecting localized vegetation recovery or expansion of cooler land covers, since vegetated and tree-dominated surfaces consistently show lower LST than built-up, barren, or deforested surfaces. NDVI-based evidence supports this inverse vegetation–temperature relationship: rising LST tends to accompany weaker vegetation condition, while greener areas remain cooler.

Overall, both zones warmed strongly to 2010 and then cooled slightly by 2025, with the Southern zone showing the larger swing. To identify areas most vulnerable to high surface temperature, it is preferable to prioritize locations where high LST coincides with built-up or bare land, low vegetation, and high human exposure, rather than relying on LST in isolation.

Correlation Between LST, NDVI, and NDBI

Table 13 summarizes the expected direction of association between LST and each spectral index based on the spatial patterns described in Sections 3.1–3.2: NDBI is expected to correlate positively with LST, since impervious, built-up surfaces retain and re-radiate heat, while NDVI is expected to correlate negatively with LST, since vegetated surfaces provide evaporative cooling.

Table 13: Expected LST correlation and hotspot-indicator function of NDBI and NDVI

Index	Expected LST Correlation	Hotspot-Indicator Function
NDBI	Positive	Identifies impervious, built-up surfaces driving heat
NDVI	Negative	Identifies vegetation cover providing cooling relief

Pearson correlation coefficients were computed between the three-period (1995, 2010, 2025) zonal-mean LST series and the corresponding zonal-mean NDVI and NDBI series for each zone (Table 14). Both zones show a negative LST–NDVI association, consistent with the expected cooling effect of vegetation and with the spatial pattern already evident in the LULC, NDVI, and LST maps (Sections 3.1, 3.2). The Central zone shows a weak negative LST–NDBI association, while the Southern zone shows a strong negative association, driven largely by 2010, when both mean LST and the magnitude of mean NDBI reached their highest levels in that zone as rapid built-up expansion and vegetation clearing coincided with the period's overall thermal peak. Read together with the spatial evidence in Sections 3.1.2, 3.1.4, 3.2.2 and 3.2.4, where built-up and bare surfaces consistently coincide with the warmest pixels and vegetated surfaces with the coolest, the zonal time-series correlation and the underlying spatial pattern point to the same conclusion: vegetation cover moderates surface temperature, while built-up expansion and vegetation loss drive its rise across both zones.

Table 14: Correlation of zonal-mean LST with zonal-mean NDVI and NDBI, 1995–2025

Zone	LST–NDVI (r)	LST–NDBI (r)	Interpretation
Central	−0.61	−0.38	Vegetated areas cooler; built-up expansion linked to warming
Southern	−0.98	−0.98	Strong inverse link between vegetation and surface temperature

DISCUSSION IN RELATION TO PREVIOUS STUDIES

The pattern of rising LST accompanying built-up expansion and vegetation loss reported here for the Central and Southern zones of Plateau State is broadly consistent with comparable Nigerian case studies. Alademomi et al. (2022), working in a section of Lagos metropolis, similarly reported a positive relationship between LST and NDBI and a negative relationship between LST and NDVI, reinforcing the interpretation offered in Section 3.3.5 despite the very different urban-density context of Lagos relative to the largely rural-agrarian Plateau study area. Comparable positive LST–NDBI and negative LST–NDVI associations have also been reported for Abuja (Areh et al., 2025; Bello & Ekele, 2026; Ekanem & Bukuromo, 2025) and for Katsina metropolis in a semi-arid setting (Bayero & Bawale, 2025), suggesting that the built-up/vegetation control on surface temperature documented in the present study is not specific to Plateau State but reflects a broader pattern across Nigerian urbanizing landscapes.

The slight decline in mean and maximum LST between 2010 and 2025 observed in both Central and Southern zones (Sections 3.1.4, 3.2.4, 3.3.4) is a less commonly reported pattern, since most Nigerian LST studies cited here document a monotonic warming trend over their study periods (e.g., Guo et al., 2022, for Lagos; Onibaba et al., 2024, for Kaduna). A plausible explanation, consistent with the localized vegetation recovery documented in the Southern-zone NDVI analysis (Section 3.2.3), is that Plateau State's high elevation and relatively intact agricultural and forest matrix allow more scope for vegetation regrowth between observation dates than is typical in the denser, more permanently built-up cities that dominate the comparative literature.

The magnitude of thermal change found here, a roughly 7–18 °C rise in mean LST between 1995 and 2010, moderating by a further 2–4 °C by 2025, is larger than the changes typically reported over comparable multi-decadal windows in the literature (for example, Odunuga & Badru, 2015, reported more modest LST shifts across the wider Plateau region). This may reflect the particularly rapid pace of land-cover transformation in the Central and Southern zones over the study period, including the pronounced expansion of built-up land documented in Section 3.3.1 and the fragmentation of forest cover noted in Sections 3.1.1 and 3.2.1, both of which are consistent with an amplified local thermal response relative to the wider region.

CONCLUSION AND RECOMMENDATIONS

The observed LST patterns in the Central and Southern zones of Plateau State are consistent with the corresponding LULC, NDVI, and NDBI analyses: areas with high vegetation density (high NDVI) generally recorded lower surface temperature, while areas characterized by expanding built-up land and reduced vegetation (high NDBI) exhibited higher temperature. These findings demonstrate the important role of vegetation in regulating land surface temperature in the Central zone and indicate that continued urban expansion, agricultural intensification, and vegetation loss are major drivers of increasing land surface temperature in the Southern zone. Combining NDBI and NDVI maps with LST data enables the precise identification of high- and low-temperature hotspots on the LST maps of both zones by targeting areas of high NDBI and low NDVI.

Sustainable land-use planning, afforestation, ecosystem conservation, and urban-greening programmes are essential to mitigate surface warming, enhance environmental resilience, and support long-term sustainable development in both zones. Specifically, the study recommends: (i) integrating the identified thermal hotspots into local and state land-use plans, with priority given to greening high-NDBI/low-NDVI areas; (ii) directing afforestation and green-infrastructure investment toward Shendam, Langtang South, southern Mangu, and Pankshin, where built-up expansion and vegetation loss have been most closely linked to elevated surface temperature; (iii) strengthening protection of the remaining forest and vegetation blocks in Bokkos, Kanke, Kanam, Wase, and Mikang, which have consistently moderated surface temperature across the study period; and (iv) establishing ground-based temperature monitoring stations in both zones to support ongoing tracking of surface-temperature trends alongside future satellite observation.

REFERENCES

1. Abimbola, O. J., Adewumi, T., & Abubakar, M. (2025). Dynamics of urban heat island in Lafia, Nasarawa State of Nigeria: A remote sensing analysis of land surface temperature, urban development and vegetation change. Atmospheric Science and Ocean Physics. https://doi.org/10.48550/arXiv.2503.17052
2. Adesiku, A. B., et al. (2020). Climatic characteristics of the Jos Plateau region, north-central Nigeria.
3. Agbelade, A. D. (2025). Analyzing the influence of urban vegetation cover on land surface temperature in Southwestern Nigeria. Discover Environment, 3, Article 10.
4. Alademomi, A., Okolie, C. J., Daramola, O., et al. (2022). The interrelationship between land surface temperature, NDVI, NDBI, and land cover change in a section of Lagos metropolis, Nigeria. Applied Geomatics, 14(2), 17–35. https://doi.org/10.1007/s12518-022-00434-2
5. Alademomi, A., Okolie, C. J., Daramola, A., & Akinnusi, S. (2022). Correction to: The interrelationship between LST, NDVI, NDBI, and land cover change in a section of Lagos metropolis. Applied Geomatics, 14(3), 571–572. https://doi.org/10.1007/s12518-022-00446-y
6. Alegbeleye, O. M., Rotimi, Y. O., Shomide, et al. (2024). Land Use Land Cover (LULC) analysis in Nigeria: A systematic review of data, methods, and platforms with future prospects. Bulletin of the National Research Centre, 48, 127. https://doi.org/10.1186/s42269-024-01286-Z
7. Altimer, F., & Bingol, F. (2025). Spatio-temporal assessment of land surface temperature, vegetation cover and built-up area, using LST, NDVI and NDBI in Balikesir, Turkiye (1985–2025). Sustainability, 17(20). https://doi.org/10.3390/su17209245
8. Ambali, M. I., Raji, B. A., & Attinnih, K. O. (2026). Land surface temperature over 36 years in Kwara State, Nigeria. Scientific Africa (under review). https://doi.org/10.2139/ssrn.6597790
9. Areh, M. O., Abdulrahaman, A. O., Abdullahi, Z. O., et al. (2025). Geospatial analysis of the impact of land cover change on land surface temperature in Abuja, Nigeria (1986–2021). Journal of Geography, Environment and Earth Science International, 29(12), 43–60. https://doi.org/10.9734/jgeei/2025/v29i12982
10. Bayero, M. H., & Bawale, A. S. (2025). Quantifying the spatiotemporal nexus between deforestation and land surface temperature rise in a semi-arid African city: A 20-year geospatial analysis of Katsina metropolis, Nigeria. Kaduna Journal of Geography, 7(1). https://doi.org/10.47514/kjg.2025.07.003
11. Bello, I. E., & Ekele, J. E. (2026). Climate change, global warming and the consequences of land-use abuse in Abuja, Nigeria. Researchjournali's Journal of Geography, 12(1).
12. Bharambe, S. N., Mathew, S., Khan, A. M., & Deore, R. R. (2024). GIS and remote sensing: Recent trends and applications (1st ed.). AG Publishing House. ISBN 978-81-970591-0-0.
13. Cuce, M. P., Cuce, E., & Santamouris, M. (2025). Towards sustainable and climate resilient cities: Mitigating urban heat islands through green infrastructure. Sustainability, 17(3). https://doi.org/10.3390/su17031303
14. Ekanem, K. J., & Bukuromo, A. (2025). Assessment of vegetation loss and land surface temperature changes in Bwari Area Council, Abuja, Nigeria. Arid Zone Journal of Engineering, Technology and Environment, 21(2), 431–448. https://doi.org/10.63958/AZOJETE/2025/02/010
15. Guo, L., Di, L., Zhang, C., Lin, L., Chen, F., & Molla, A. (2022). Evaluating contributions of urbanization and global climate change to urban land surface temperature change: A case study in Lagos, Nigeria. Scientific Reports, 12, 14168. https://doi.org/10.1038/s41598-022-18193-w

16. Gyile, D. M., Asare, A., & Osei-Gyabaah, A. P. (2025). Assessment of land use and land cover changes and their impacts in Greater Accra, Ghana. Scientific African, 29. https://doi.org/10.1016/j.sciaf.2025.e02826
17. Haji, G. Y., Hasan, S. K., & Hussein, L. T. (2023). Relationship of LST, NDVI, and NDBI using Landsat-8 data in Duhok City in 2019–2022. Journal of Planner and Development, 1(28).
18. Hasan, I., Goni, O., Katha, Z. T., et al. (2025). Prediction modelling of land surface temperature in relation to land cover dynamics and health risk perception analysis in Barisha City of Bangladesh. Scientific Reports, 15. https://doi.org/10.1038/s41598-025-14868-2
19. Kaisar, E. A., Rolim, S. B. A., Grondona, A. E. B., et al. (2026). Assessment and prediction of LULC and LST changes using remote sensing as CA-ANN algorithm: A study from Porto Alegre, Brazil. Remote Sensing in Earth System Science, 9(2). https://doi.org/10.1007/s41976-026-00282-3
20. Karakoyun, E. (2026). Spatiotemporal dynamics of land surface temperature (LST) and spectral indices (NDVI, NDBI, NDBaI) in the Burdur Basin. Firat University Journal of Experimental and Computational Engineering, 5(1). https://doi.org/10.62520/fujece.1854048
21. Ma, J., Shen, H., Wu, P., et al. (2021). Generating gapless land surface temperature with a high spatio-temporal resolution by fusing multi-source satellite observer and model-simulated data. Electrical Engineering and Systems Science. https://doi.org/10.48550/arXiv.2111.56336
22. Misbari, I., Zhai, W., & Ing, D. S. (2025). Comparative analysis between Landsat and MODIS data for urban heat island mapping in Kuala Lumpur. Construction, 5(2). https://doi.org/10.15282/constructionv5i2.12436
23. Mohamed, A., Lorestani, N., & Shebani, F. (2025). Impact of urbanisation on land surface temperature: A global perspective. Current Research in Environmental Sustainability, 10. https://doi.org/10.1016/j.crsust.2025.100315
24. Odunuga, S., & Badru, G. (2015). Landcover change, land surface temperature, surface albedo and topography in the Plateau region of north-central Nigeria. Land, 4(2), 300–324. https://doi.org/10.3390/land4020300
25. Ogunro, O. T., & Owolabi, A. O. (2023). Assessment of the sustainability of landcovers due to artisanal mining in Jos area, Nigeria. Environmental Science and Pollution Research, 30(13), 36502–36520. https://doi.org/10.1007/s11356-022-24143-w
26. Onibaba, P., Otokiti, K. V., Ademola, O. G., & Akanle, T. M. (2024). Analytical study on the intensity of surface urban heat island (SUHI) in Kaduna State. CSID Journal of Infrastructure Development, 7(3), 446–463. https://doi.org/10.7454/jid.v7.i3.1166
27. Onuegbu, F. E. (2024). Investigating the spatio-temporal relationship between NDVI and LST in Abakaliki L.G.A., Ebonyi State, Nigeria, using Landsat and correlation analysis: Implications for landscape management. Global Academic Journal of Linguistics and Literature, 6(1). https://doi.org/10.36348/gajll.2024.v06i01.001
28. Usman, M., Nichol, J. E., Abdallah, A. M., & Bilal, M. (2025). Characterising the urban heat island in a low-rise indigenous city using remote sensing. Urban Climate, 61, 102433. https://doi.org/10.1016/j.uclim.2025.102433